

# Who ate whom: Population dynamics with age-structured predation

David Goluskin

15 October 2010

## Abstract

We study a population model in which there are two species, one of which has a juvenile and adult life stage. The adults of the first species prey on the second species, which in turn preys on the juveniles of the first. One version of the model represents systems where neither species can survive on its own, although we find that both can survive through mutual predation. To avoid extinction, the two types of predation must be of sufficient strength and in appropriate proportion to one another. Another version of the model represents systems where each species can survive without the other, and there we find that mutual predation is capable of increasing both of their equilibrium populations or creating stable limit cycles.

## 1 Introduction

An organism's trophic level is the position that it occupies in the food web, defined by the organisms that it eats and vice versa. However, few organisms occupy the same trophic levels throughout their lives. Typically an organism's predators and prey change over its lifetime, as do the organisms of similar trophic level with which it competes for food. Werner and Gilliam [2] review many examples of ecosystems in which competitive and predatory relationships are age- and size-dependent. As an instance of the latter, adult salamanders and newts prey on one another's juveniles. Similarly, frogs eat insects, while insect larva eat tadpoles. Although competition is important, we do not consider it in this report, where our object is to explore solely the dynamics that arise in ecological models with age-structured predation.

## 2 Development of the models

Any model for age-structured predation must have at least two species, and at least one of the species must have multiple life stages. Some ecological models have used continuous age or size variables to describe life stage, which requires partial differential equations to describe the change of populations in time, but the simplest possibility is to have two discrete life stages. Thus, the simplest possible model has three populations in total: one species with one life stage and one species with both juvenile and adult life stages. For concreteness we shall call our populations tadpoles ( $T$ ), frogs ( $F$ ), and insects ( $I$ ), where the frogs eat the insects, the insects eat the tadpoles, and the tadpoles and frogs beget one another through recruitment and reproduction. For simplicity we shall assume that recruitment occurs at a rate proportional to tadpole biomass, that

# Report Documentation Page

Form Approved  
OMB No. 0704-0188

Public reporting burden for the collection of information is estimated to average 1 hour per response, including the time for reviewing instructions, searching existing data sources, gathering and maintaining the data needed, and completing and reviewing the collection of information. Send comments regarding this burden estimate or any other aspect of this collection of information, including suggestions for reducing this burden, to Washington Headquarters Services, Directorate for Information Operations and Reports, 1215 Jefferson Davis Highway, Suite 1204, Arlington VA 22202-4302. Respondents should be aware that notwithstanding any other provision of law, no person shall be subject to a penalty for failing to comply with a collection of information if it does not display a currently valid OMB control number.

1. REPORT DATE <b>15 OCT 2010</b>		2. REPORT TYPE		3. DATES COVERED <b>00-00-2010 to 00-00-2010</b>	
4. TITLE AND SUBTITLE <b>Who ate whom: Population Dynamics With Age-structured Predation</b>				5a. CONTRACT NUMBER	
				5b. GRANT NUMBER	
				5c. PROGRAM ELEMENT NUMBER	
6. AUTHOR(S)				5d. PROJECT NUMBER	
				5e. TASK NUMBER	
				5f. WORK UNIT NUMBER	
7. PERFORMING ORGANIZATION NAME(S) AND ADDRESS(ES) <b>Woods Hole Oceanographic Institution, Woods Hole, MA, 02543</b>				8. PERFORMING ORGANIZATION REPORT NUMBER	
9. SPONSORING/MONITORING AGENCY NAME(S) AND ADDRESS(ES)				10. SPONSOR/MONITOR'S ACRONYM(S)	
				11. SPONSOR/MONITOR'S REPORT NUMBER(S)	
12. DISTRIBUTION/AVAILABILITY STATEMENT <b>Approved for public release; distribution unlimited</b>					
13. SUPPLEMENTARY NOTES <b>See also ADA544302</b>					
14. ABSTRACT <b>We study a population model in which there are two species, one of which has a juvenile and adult life stage. The adults of the first species prey on the second species which in turn preys on the juveniles of the first. One version of the model represents systems where neither species can survive on its own, although we find that both can survive through mutual predation. To avoid extinction, the two types of predation must be of sufficient strength and in appropriate proportion to one another. Another version of the model represents systems where each species can survive without the other, and there we find that mutual predation is capable of increasing both of their equilibrium populations or creating stable limit cycles.</b>					
15. SUBJECT TERMS					
16. SECURITY CLASSIFICATION OF:			17. LIMITATION OF ABSTRACT	18. NUMBER OF PAGES	19a. NAME OF RESPONSIBLE PERSON
a. REPORT <b>unclassified</b>	b. ABSTRACT <b>unclassified</b>	c. THIS PAGE <b>unclassified</b>			

reproduction occurs at a rate proportional to frog biomass, and that a constant fraction of the biomass being transferred through predation is lost to metabolic inefficiencies. The model as described thus far is diagrammed in Figure 1. Through the “feeding/death” fluxes in Figure 1, each population may gain biomass by feeding on the external environment (which excludes the other two populations explicitly modeled), or lose biomass through death. All that remains to fully define our population model is to specify the functional forms of the predation and feeding/death terms.

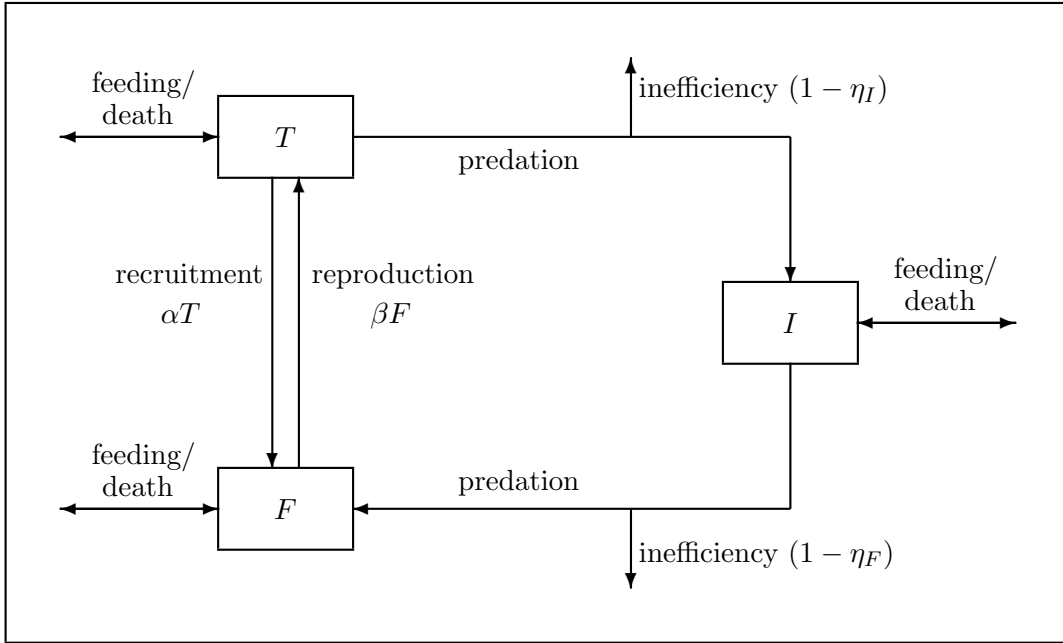


Figure 1: Biomass flux in the tadpole-frog-insect system.

## 2.1 Feeding or death terms

Assuming the tadpoles, frogs, and insects do not compete with one another, each population’s feeding/death term should be independent of the other two populations. The simplest choice is a proportional law, which in the absence of predation creates exponential growth or decay, depending on the parameter values. Unbounded exponential growth is unrealistic, but exponential decay is feasible: it represents a case where the two species cannot survive without predation, and we analyze such a model in Section 3. We also wish to consider a scenario in which both species would survive without the predation. This requires that the system have carrying capacities, which cause initially exponential growth to saturate at finite values. We must put a carrying capacity on the insects, but we have a choice between putting one on the frogs, the tadpoles, or both. We shall somewhat arbitrarily place a carrying capacity on frogs and not on tadpoles. In the biological reality of frogs and tadpoles this is usually accurate; frogs will typically run out of environmental resources before tadpoles do. But for other species, resources may certainly be scarcer for juveniles than for adults. We analyze the carrying capacity model in Section 4.

## 2.2 Predation terms

The simplest possible predation law is a quadratic one in which the rate of predation is proportional to both predator and prey populations, the so-called Holling type I functional form [1]. Some models of age-structured predation employing these forms were studied by Whitehead and Doering [3], but such a form fails to reflect the fact that increasing the amount of prey beyond a certain point stops benefiting the predators because there is a limit to how fast they can eat and metabolize the prey. The Holling type II functional form avoids this problem by saturating as the amount of prey becomes large:

$$\text{rate of predation} = C_1 \frac{(\text{prey population})(\text{predator population})}{1 + C_2(\text{prey population})},$$

where  $C_1$  and  $C_2$  are constant parameter. We have examined some models employing the type I form, but it leads to unbounded growth in certain cases, so we shall henceforth always use the type II form. It is not hard to justify needing a predation law with saturation, but it is certainly not clear *a priori* that the type II form is the best choice. We justify this choice in the appendix, where we derive the type II form as an asymptotic limit of a higher-dimensional dynamical system and numerically compare the reduced system with the higher-dimensional system.

## 3 Model without carrying capacities

Let the feeding/death term for tadpoles add biomass at the rate  $\epsilon_T T$ , where  $\epsilon_T$  can take either sign, and likewise for frogs and insects. Then, the dimensional ODE governing the biomass of each population is

$$\dot{T} = -\gamma T + \beta F - \kappa \frac{IT}{1 + \mu T} \quad (1)$$

$$\dot{F} = \alpha T - \zeta F + \eta_F \lambda \frac{FI}{1 + \nu I} \quad (2)$$

$$\dot{I} = \epsilon_I I + \eta_I \kappa \frac{IT}{1 + \mu T} - \lambda \frac{FI}{1 + \nu I}, \quad (3)$$

where

$$\begin{aligned} \gamma &= \alpha - \epsilon_T \\ \zeta &= \beta - \epsilon_F. \end{aligned}$$

Without frogs or insects, tadpoles should die out, and likewise for frogs, so  $\gamma$  and  $\zeta$  must be positive. Only the  $\epsilon_I$  parameter may be negative. If  $\alpha < \gamma$ , tadpole feeding is adding biomass to the system, and the same is true for frogs if  $\beta < \zeta$ . The parameters  $\eta_I$  and  $\eta_F$  are metabolic efficiencies, so they must fall between 0 and 1. We now nondimensionalize the system by

$$t \mapsto \frac{1}{\gamma} t \quad T \mapsto \frac{1}{\mu} T \quad F \mapsto \frac{\gamma}{\beta \mu} F \quad I \mapsto \frac{1}{\nu} I. \quad (4)$$

This particular nondimensionalization is attractive because it retains unique coefficients on all the nonlinear predation terms and minimizes the number of free parameters (seven). Its drawback is that the different populations are no longer in equivalent units of biomass, so they cannot be meaningfully compared. This is tolerable because we are more interested in qualitative system behavior than relative population biomasses. The

nondimensional ODE is

$$\dot{T} = -T + F - d \frac{IT}{1+T} \quad (5)$$

$$\dot{F} = aT - bF + g \frac{FI}{1+I} \quad (6)$$

$$\dot{I} = cI + e \frac{IT}{1+T} - f \frac{FI}{1+I}, \quad (7)$$

where

$$\begin{aligned} a &= \frac{\alpha\beta}{\gamma^2} \\ b &= \frac{\zeta}{\gamma} \\ c &= \frac{\epsilon I}{\gamma} \\ d &= \frac{\kappa}{\gamma\nu} \\ e &= \frac{\eta I \kappa}{\gamma\mu} \\ f &= \frac{\lambda}{\beta\mu} \\ g &= \frac{\eta F \lambda}{\gamma\nu}. \end{aligned}$$

### 3.1 Model without predation

Without predation, the model is linear, and the  $T$ - $F$  system decouples from the insects:

$$\frac{d}{dt} \begin{pmatrix} \Delta T \\ \Delta F \\ \Delta I \end{pmatrix} = \begin{pmatrix} -1 & 1 & 0 \\ a & -b & 0 \\ 0 & 0 & c \end{pmatrix} \begin{pmatrix} \Delta T \\ \Delta F \\ \Delta I \end{pmatrix}.$$

The tadpoles and frogs decay exponentially if  $a < b$  and grow exponentially if  $a > b$ , while the insects decay exponentially if  $c < 0$  and grow exponentially if  $c > 0$ . The behaviors of the uncoupled systems split the full system rather naturally into four separate cases. (Structurally unstable parameter values such as  $a = b$  or  $c = 0$  will not be considered in anything that follows.) The only equilibrium of this system is the origin, and the decoupled systems are rather boring without predation. Predation can create stable fixed points and limit cycles for all four combinations of signs of  $(a - b)$  and  $c$ , but only the case in which the  $T$ - $F$  and  $I$  systems both decay without predation is biologically reasonable, so we shall restrict ourselves to this case. Henceforth in this section,  $a < b$  and  $c < 0$ .

When  $I$  and the  $T$ - $F$  system both decay without predation, the mechanism by which predation can stabilize the system is the following. Suppose that biomass enters the system through frog feeding ( $\zeta < \beta$ ) and leaves the system through tadpole death ( $\gamma > \alpha$ ), with tadpole death dominating when the  $T$ - $F$  system is isolated. In other words, the rate of reproduction is higher than ideal. Introducing insects creates a flux of biomass from tadpoles to frogs, where it is used to create more biomass from external feeding, rather than lost to tadpole death. This effect can prevent the entire system from decaying to zero, even with the additional sources of biomass loss by insect death and metabolic inefficiencies.

### 3.2 Lyapunov bound

Not only is the origin linearly stable when  $a < b$  and  $c < 0$ , the Lyapunov functional  $L \equiv \frac{\epsilon}{d}T + \frac{f}{g}F + I$  suffices to show that all solutions decay to the origin. This is a rather

narrow range of validity, but it suggests the possible importance of the ratio  $\frac{eg}{df}$ . In terms of dimensional variables,

$$\frac{eg}{df} = \eta_I \eta_F \frac{\beta}{\gamma}.$$

Biologically,  $\eta_I \eta_F$  is the squared geometric mean of the metabolic efficiencies, so we can think of this term roughly as the metabolic efficiency of the entire system.

### 3.3 Nontrivial equilibria

At nontrivial fixed points,

$$F = T \left( 1 + \frac{dI}{1+T} \right) \quad (8)$$

$$aT = F \left( b - \frac{gI}{1+I} \right) \quad (9)$$

$$0 = c + \frac{eT}{1+T} - \frac{fF}{1+I}. \quad (10)$$

From Equation (8),  $I$  and  $T$  uniquely define  $F$  at a fixed point. Using this equation to eliminate  $F$  from the latter two yields two polynomial equations in  $I$  and  $T$ :

$$a(1+I)(1+T) = (1+T+dI)(b+bI-gI) \quad (11)$$

$$c(1+I)(1+T) + eT(1+I) = fT(1+T+dI). \quad (12)$$

Equation (11) is linear in  $T$ , and Equation (12) is linear in  $I$ , so they may be used to find explicit expressions for  $T(I)$  and  $I(T)$ , respectively:

$$T = \frac{dI(b+(b-g)I)}{(a+g-b)I+a-b} - 1$$

$$I = \frac{fT^2 - (c+e-f)T - c}{(c+e-df)T+c}.$$

Evidently,  $I$  and  $T$  define one another uniquely. Applying  $T(I)$  to Equation 12 gives a cubic polynomial for  $I$  at the equilibria, so there are at most three positive real population equilibria.

$$i_3 I^3 + i_2 I^2 + i_1 I + i_0 = 0, \text{ where}$$

$$i_0 = -e(a-b)^2 < 0$$

$$i_1 = (a-b)[2e(b-g) + bd(c+e) + a(df-2e)]$$

$$i_2 = d(c+e)[(a-b)(b-g) + b(a+g-b)] - e(a+g-b)^2 + adf(a+g-b-bd)$$

$$i_3 = d(b-g)[(c+e)(a+g-b) - adf]$$

The cubic equation for  $I$  of course has explicit algebraic solutions, but they are too messy to be of use, so although we have explicit expressions for  $F$  and  $T$  in terms of  $I$ , we cannot generally predict whether  $F$  and  $T$  will be positive when  $I$  is positive. The best we can do analytically is infer some partial information about the signs of polynomial roots. For this, we also need the first and last coefficients of the cubic polynomial governing  $T$ , which we derive by applying  $I(T)$  to Equation 11:

$$t_3 T^3 + t_2 T^2 + t_1 T + T = 0, \text{ where}$$

$$T = -c^2 g < 0$$

$$t_3 = f[(c+e)(a+g-b) - adf].$$

**Theorem** Let  $a < b$  and  $c < 0$ . If  $g < b$  and  $adf < (c + e)(a + g - b)$ , there are either 1 or 3 positive equilibria. Otherwise, there are either 0 or 2 positive equilibria.

**Proof** The  $I$  polynomial is cubic, and  $I$  uniquely defines  $F$  and  $T$ , so there are at most three real, positive equilibria. It is clear from Equation 8 that  $F$  is positive when  $I$  and  $T$  are, so it suffices to know when the  $I$  and  $T$  polynomials have corresponding positive roots. There are three ways in which the number of positive roots of the  $I$  or  $T$  polynomials may change. Firstly, a root may remain real but leave the positive octant if  $i_0$  or  $t_0$  becomes negative, but we have eliminated this possibility by assumption. Secondly, the number of positive equilibria may change by two when a pair of equilibria become complex simultaneously, a saddle-node bifurcation. Thirdly, an equilibrium may move off to infinity when  $i_3$  or  $t_3$  pass through zero. By dividing parameter space into four regions in which  $i_3$  and  $t_3$  do not change sign, we are assured that the number of equilibria within each region may change only by saddle-node bifurcations. These regions are

$$\begin{aligned} I &\equiv \{i_3 > 0, t_3 > 0\} = \{g < b, adf < (c + e)(a + g - b)\} \\ II &\equiv \{i_3 < 0, t_3 > 0\} = \{g > b, adf < (c + e)(a + g - b)\} \\ III &\equiv \{i_3 > 0, t_3 < 0\} = \{g < b, adf > (c + e)(a + g - b)\} \\ IV &\equiv \{i_3 < 0, t_3 < 0\} = \{g > b, adf > (c + e)(a + g - b)\}. \end{aligned}$$

If we know the number of positive equilibria at one point in each parameter region, we know the number of positive equilibria at all points in that parameter region, modulo 2. So, we chose one such test point in each parameter region and computed the equilibria numerically, inferring from this the possible number of positive equilibria in each parameter region. The results are tabulated in Table 1. Evidently, there may be 1 or 3 positive equilibria in parameter region I, and 0 or 2 otherwise. Parameter region I is defined precisely by the condition that  $g < b$  and  $adf < (c + e)(a + g - b)$ , so the theorem is proved. ■

Table 1: Number of nontrivial equilibria in each of the four parameter regions, as inferred from a test points,  $(a, b, c, d, e, f, g)$ , in parameter space.

Parameter region	Test point	Number of positive equilibria at test point	Number of positive equilibria in region
$I$	$(0.9, 1, -0.5, 1, 1.5, 0.1, 0.5)$	1	1 or 3
$II$	$(0.9, 1, -0.5, 1, 1.5, 0.1, 2)$	2	0 or 2
$III$	$(0.9, 1, -0.5, 100, 1.5, 0.1, 0.5)$	0	0 or 2
$IV$	$(0.9, 1, -0.5, 100, 1.5, 0.1, 2)$	0	0 or 2

By the preceding theorem, we have partial information about the number of equilibria inside and outside region I. Because a saddle-node bifurcation creates two equilibria of opposite stability, we also know that there can be at most two stable equilibria inside parameter region I, and at most one stable equilibrium outside it. We would of course like precise conditions on when the saddle-node bifurcations occur, thereby further dividing our parameter regions into ones in which the numbers of positive equilibria are exactly known. This requires knowing when  $I$  or  $T$  become complex. Since  $I$  and  $T$  are

governed by cubic equations, this can in principle be determined from the discriminants of those equations. The  $I$  equation has one real and two complex roots precisely when

$$\Delta_I \equiv 18i_3i_2i_1i_0 - 4i_2^3i_0 + i_2^2i_1^2 - 4i_3i_1^3 - 27i_3^2i_0^2 < 0,$$

and likewise for the coefficients of the  $T$  equation, so the parameter regimes we seek are divided by the surfaces on which the discriminants vanish. Unfortunately, these inequalities are prohibitively messy when expressed in terms of the problem parameters. In biological modeling, one is more interested in qualitative behaviors than the precise values at which bifurcations occur, so we will be content to observe the saddle-node bifurcations numerically.

### 3.4 Numerical exploration of parameter space

Asymptotic analysis shows that the predation parameters cannot be small compared to the population decay rates if predation is to stabilize the decay. In fact, numerical experiments reveal that the predation parameters must typically be about an order of magnitude larger than the decay rates. In light of this, we shall fix  $(a, b, c) = (0.9, 1, -0.1)$  and expect interesting behavior when predation parameters are  $O(1)$ .

#### 3.4.1 Looking for bifurcations

When  $(d, e, f, g) = (0.2, 1, 0.2, 0.5)$ , there are three positive equilibria, the maximum number possible, so we choose this as a starting point from which to explore the four-dimensional space of predation parameters. Linearizing the system about these equilibria and computing matrix eigenvalues numerically, we find that none of the fixed points are stable. Biologically, we are interested in regimes where there are stable fixed points, so we use the bifurcation continuation package MATCONT to continue these equilibria in parameter space. Arbitrarily choosing the parameter  $e$  in which to continue the equilibria, we obtain the bifurcation diagram of Figure 2. We have chosen the coordinate  $I$  for the ordinate of our bifurcation diagrams because the value of  $I$  sometimes becomes unrealistically small, and we wish to see when this is so.

Continuing in  $e$ , we find a saddle-node bifurcation ( $LP$ ), a subcritical Hopf bifurcation ( $H^+$ ), and a neutral saddle ( $NS$ ). These are all bifurcations of codimension 1, as we would expect to find when varying only one parameter. To access the higher-level structure of parameter space, we would like to find higher-codimension bifurcations. The MATCONT package can in general only find bifurcations up to codimension-2, so we shall settle for this, though ideally we would like to find bifurcations of codimension up to the dimension of our parameter space. Codimension-2 bifurcations are typically found by continuing a codimension-1 bifurcation in two parameters, so we shall continue all of the bifurcations of Figure 2. Continuing in  $e$  and  $g$  yields the bifurcation diagram of Figure 3, in which we see two types of codimension-2 bifurcations: Bogdanov-Takens bifurcations ( $BT$ ), and generalized Hopf bifurcations ( $GH$ ), also known as Bautin bifurcations. Continuing the codimension-1 bifurcations of Figure 2 in any other combination of two parameters does not yield any other types of codimension-2 bifurcations.

In the neighborhood of a Bogdanov-Takens bifurcation, there are guaranteed to be a saddle-node bifurcation and a Hopf bifurcation (both of which we have seen already), and also a saddle homoclinic bifurcation. In the neighborhood of a generalized Hopf bifurcation, there are guaranteed to be both supercritical- and subcritical Hopf bifurcations, and a fold bifurcation of limit cycles. Although we are only assured of these system behaviors in local neighborhoods of the codimension-2 bifurcations, we can reasonably expect to see them all around parameter space.



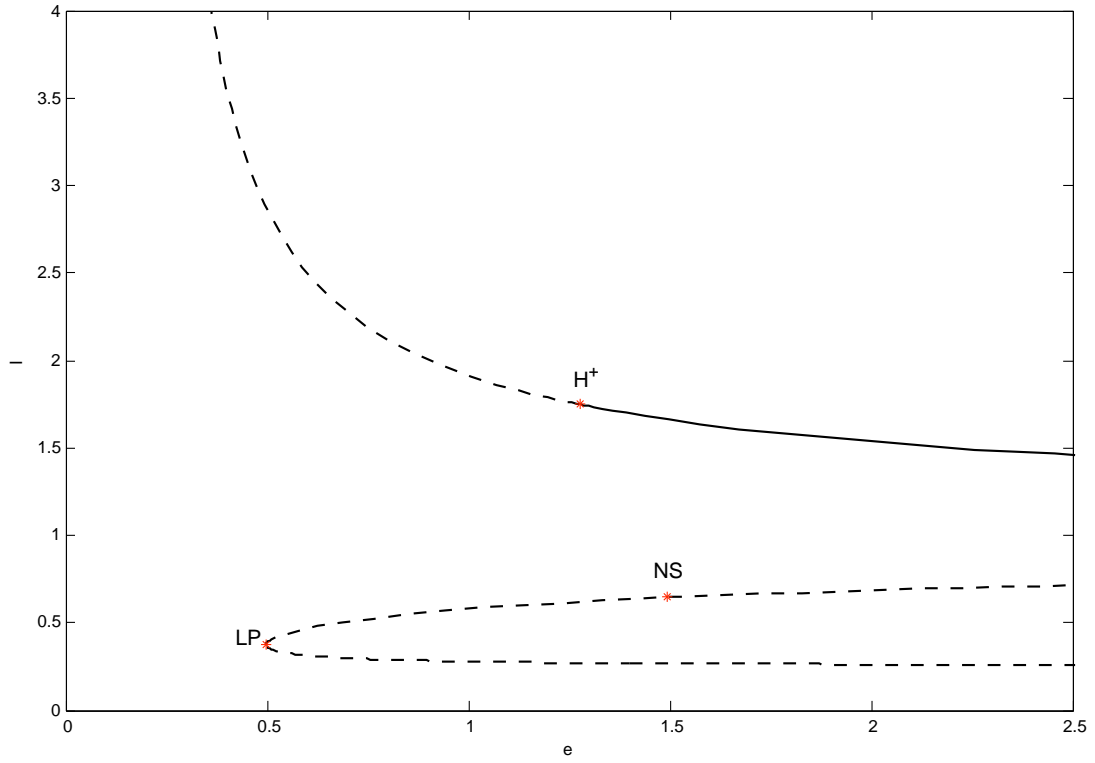


Figure 2: Continuation in  $e$  of the three starting equilibria.

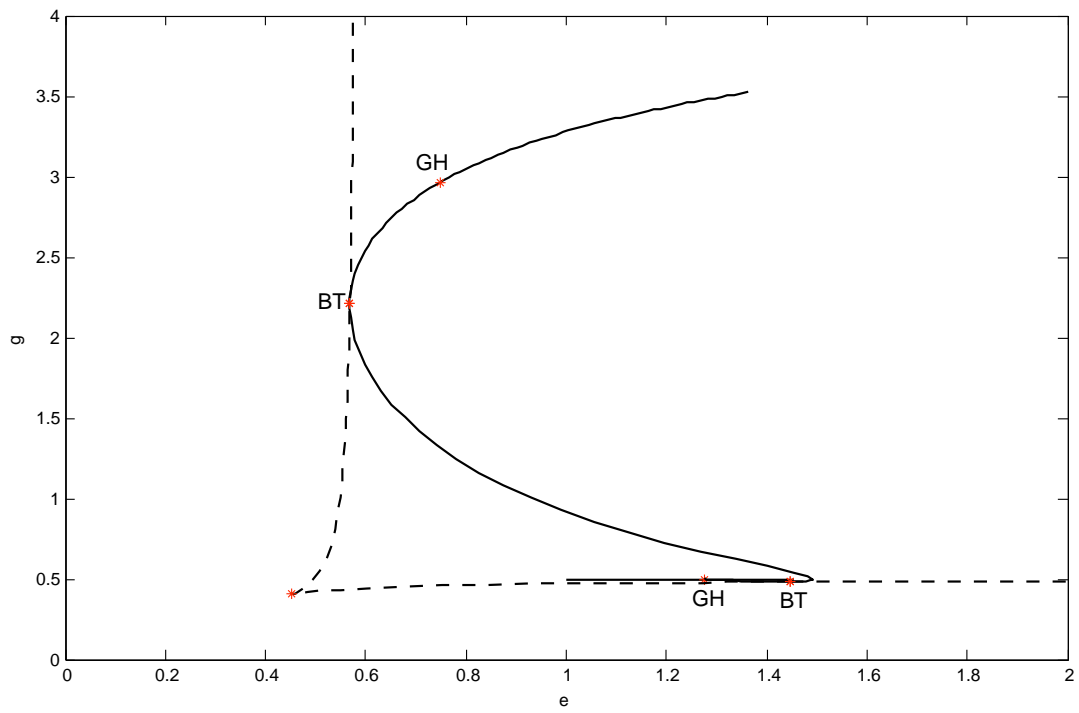


Figure 3: Continuation in  $e$  and  $g$  of the Hopf bifurcation of Figure 2.

Before exploring the effects of each parameter, we would like to find a baseline point in parameter space at which all parameters are of similar magnitude, and at which a stable fixed point exists. There is always a stable fixed point near a Hopf bifurcation, so we continue the Hopf bifurcation of Figure 2 in various pairings of the predation parameters, arriving at a point where  $(d, e, f, g)$  is near  $(2, 4, 2, 2)$ . We shall use this and other nearby values as our baseline parameter points.

### 3.4.2 Overall predation strength

To study the effect of the overall predation strength in the system, we fix the ratios between all four predation parameters and vary them proportionally. The resulting diagrams are shown in Figure 4, where we have used two slightly different parameter ratios to exhibit one case each where the Hopf bifurcation is supercritical or subcritical. In any of the bifurcation diagrams that follow, the predation parameter ratios could be chosen to realize either type of Hopf bifurcation, but the distinction is not very important because limit cycles in this system are not robust biologically, for the following reason. In the chosen regime of  $a$ ,  $b$  and  $c$ , the coordinates of the stable fixed point appear to always be such that  $I \ll T, F$ . As the limit cycle emerging from a Hopf bifurcation grows, the oscillations become strongly nonlinear, consisting of a fast part and slow part. During the slow part of the cycle, the value of  $I$  is very small. Without traveling very far in parameter space, either the limit cycle is destroyed in a homoclinic bifurcation, or  $I$  becomes so small during the slow part of the cycle that in the non-continuum of reality, the insect population would go extinct, bringing the same fate to the frogs and tadpoles. If we altered the model to include stochasticity or discrete populations, we could reasonably expect it to display this biologically-realistic extinction during such troughs of  $I$ . The type of Hopf bifurcation controls whether or not a stable limit cycle coexists with a stable fixed point, but since the limit cycle is a much less robust structure than the fixed point, the distinction is not very important.

It is evident from Figure 4 that the system has no stable fixed points or limit cycles when the predation is too weak. This is expected, since the predation must stabilize the exponential decays of the uncoupled systems, and it makes clear that predation cannot do this as a mere perturbation on the uncoupled systems. As predation increases, the fixed point not only remains stable, but its basin of attraction enlarges. Simultaneously, however, the equilibrium insect population decreases toward zero, and the frog and tadpole populations decrease asymptotically toward identical finite values. When the basin of attraction is too small, a perturbation could send the system across the separatrix and onto a trajectory heading toward the origin (extinction). When the equilibrium insect population is too small, it is vulnerable to eradication by some catastrophic event, in which fate the frogs and tadpoles would follow. The fitness of the insect population would be maximized at some intermediate predation strength that balances these two factors.

### 3.4.3 Relative strengths of the two types of predation

The parameters  $d$  and  $e$  convey the strength of the insect-tadpole predation, and the parameters  $f$  and  $g$  do likewise for the frog-insect predation. To study the effect of the relative strengths of the two types of predation, we vary the insect-tadpole predation parameters in fixed proportion while holding the other two constant, and likewise for the frog-insect parameters. The resulting bifurcation diagrams are presented in Figure 5, and they both suggest the same conclusions. The process in which insects move biomass from tadpoles to frogs is essential to stabilizing the system, and when  $I$ - $T$  predation

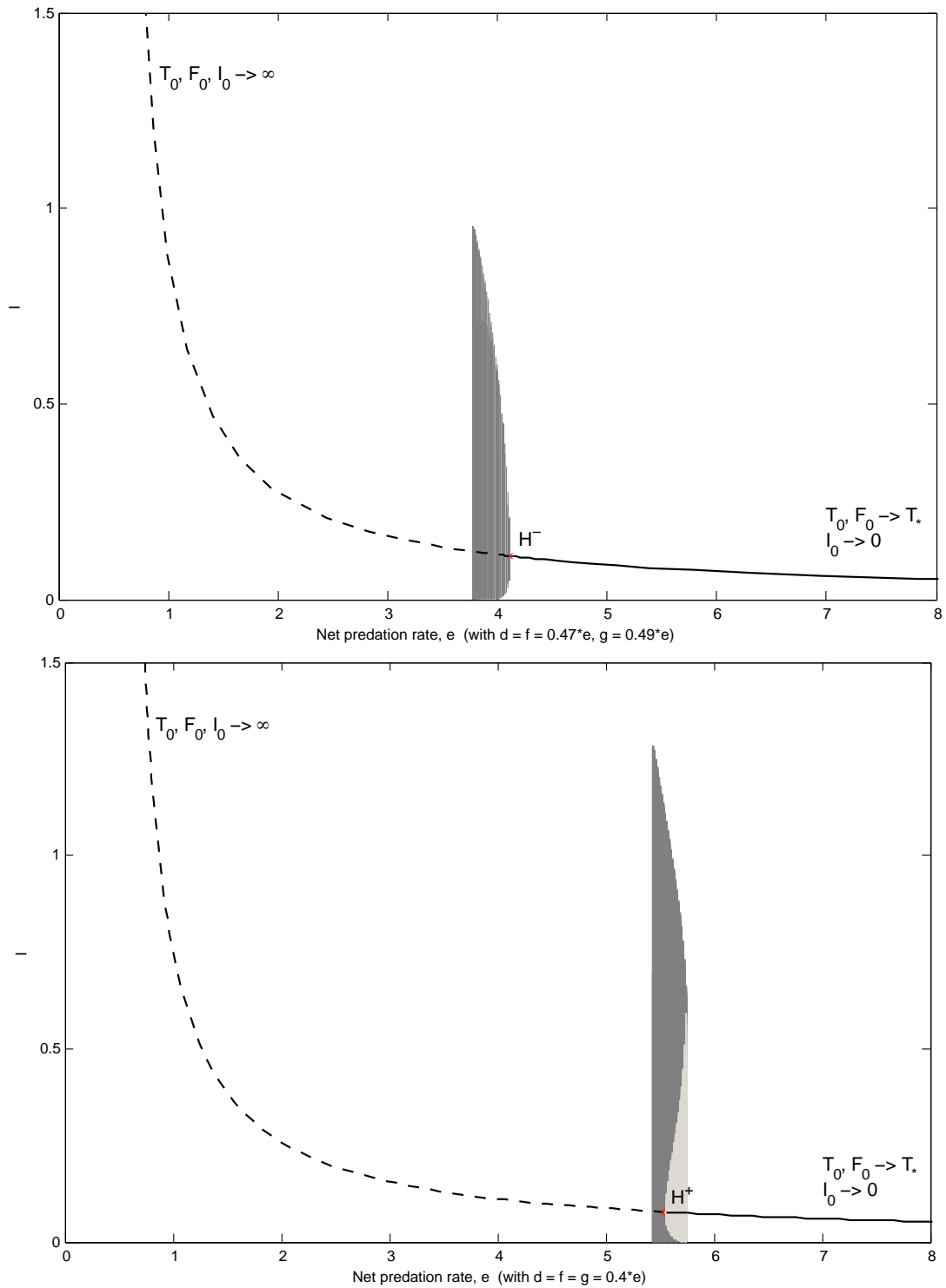


Figure 4: Bifurcation diagrams in which all four predation parameters are varied proportionally to study the overall effect of predation strength. Different proportions between the parameters can produce either supercritical (top) or subcritical (bottom) Hopf bifurcations. Light gray depicts unstable limit cycles, while dark gray depicts stable limit cycles.

is too weak relative to  $F$ - $I$  predation, the insect population is kept low and cannot transfer enough biomass, so the stable fixed point disappears through a saddle-node bifurcation. Conversely, when the  $I$ - $T$  predation is relatively strong, the fixed point will lose stability to stable oscillations. In such oscillations, insects eat tadpoles quickly and deplete the tadpole population, after which frogs eat the plentiful insects, depleting that population, and then frogs give birth to many tadpoles, losing biomass themselves until the insects rebound. When these oscillations become too dramatic, extinction is the likely result.

## 4 Model with carrying capacities

With carrying capacities on frogs and insects, the dimensional governing equations become

$$\begin{aligned}\dot{T} &= -\gamma T + \beta F - \kappa \frac{IT}{1 + \mu T} \\ \dot{F} &= \alpha T - \zeta F \left(1 + \frac{1}{N} F\right) + \eta_F \lambda \frac{FI}{1 + \nu I} \\ \dot{I} &= \epsilon_I I \left(1 - \frac{1}{M} I\right) + \eta_I \kappa \frac{IT}{1 + \mu T} - \lambda \frac{FI}{1 + \nu I}.\end{aligned}$$

### 4.1 Nontrivial equilibria

Without predation, a nontrivial equilibrium exists only if  $\frac{\alpha\beta}{\gamma\zeta} > 1$ , which is also the condition under which the origin is unstable. We wish to study a parameter regime in which the system has nontrivial behavior before predation is added, so we shall assume this inequality always holds. With predation, a nontrivial fixed point must satisfy

$$\begin{aligned}T &= \frac{1}{\alpha} F \left[ \zeta \left(1 + \frac{1}{N} F\right) - \eta_F \lambda \frac{I}{1 + \nu I} \right] \\ F &= \frac{1}{\beta} T \left( \gamma + \kappa \frac{I}{1 + \mu T} \right) \\ I &= M \left[ 1 + \frac{1}{\epsilon_I} \left( \eta_I \kappa \frac{T}{1 + \mu T} - \lambda \frac{F}{1 + \nu I} \right) \right].\end{aligned}$$

These algebraic equations cannot be solved explicitly for the equilibrium populations, so we must resort to perturbation expansions and numerical solutions.

#### 4.1.1 Perturbation of the nontrivial equilibrium by weak predation

Let the predation strength be small:

$$\kappa = \epsilon \kappa_1 \quad \lambda = \epsilon \lambda_1,$$

where  $\epsilon \ll 1$ . We can expand the equilibrium populations in  $\epsilon$  (e.g.  $T \sim T_0 + \epsilon T_1 + O(\epsilon^2)$ ), going to first order to obtain the leading order impact of predation. At zeroth order, i.e. without predation,

$$T_0 = \frac{\beta}{\gamma} \left( \frac{\alpha\beta}{\gamma\zeta} - 1 \right) N \tag{13}$$

$$F_0 = \left( \frac{\alpha\beta}{\gamma\zeta} - 1 \right) N \tag{14}$$

$$I_0 = M. \tag{15}$$

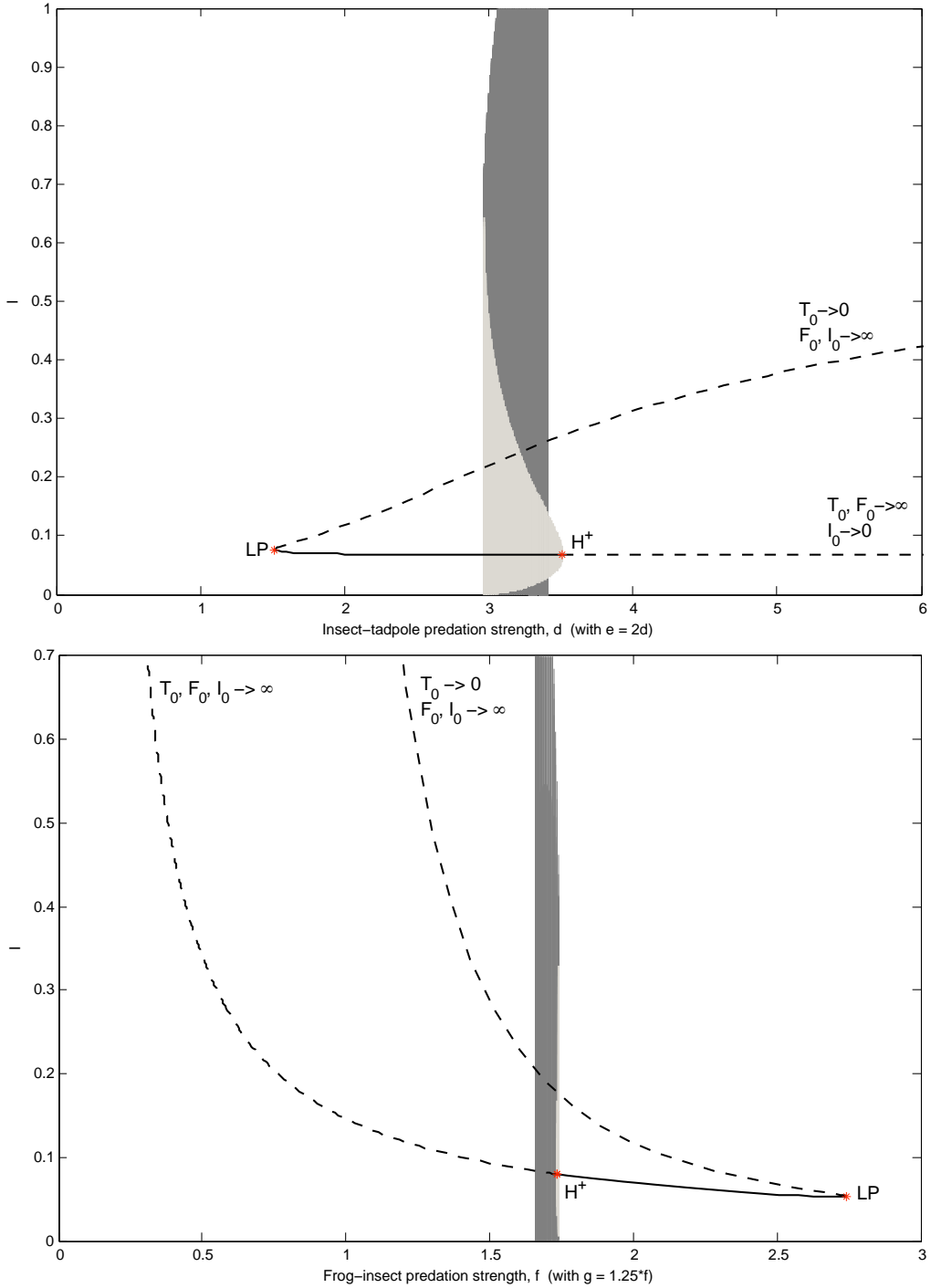


Figure 5: Bifurcation diagrams in which the relative strengths of the two types of predation are varied. To study the variation of insect-tadpole predation strength (top),  $d$  and  $e$  are varied proportionally ( $e = 2d$ ), while frog-insect predation is kept constant ( $f = 2, g = 2.5$ ). To study the variation of frog-insect predation (bottom),  $f$  and  $g$  are varied proportionally ( $f = \frac{5}{4}g$ ), while insect-tadpole predation is kept constant ( $d = 2, e = 4$ ). Light gray depicts unstable limit cycles, while dark gray depicts stable limit cycles.

The first order coefficients in the expansions are

$$\begin{aligned}
T_1 &= \frac{\beta}{\gamma} \left[ \eta_F \frac{\lambda_1}{\zeta} \frac{1}{1 + \nu M} + \frac{\kappa_1}{\gamma} \frac{(1 - 2\frac{\alpha\beta}{\gamma\zeta})}{1 + \mu\frac{\beta}{\gamma}(\frac{\alpha\beta}{\gamma\zeta} - 1)N} \right] MN \\
F_1 &= \left[ \eta_F \frac{\lambda_1}{\zeta} \frac{1}{1 + \nu M} - \frac{\kappa_1}{\gamma} \frac{\frac{\alpha\beta}{\gamma\zeta}}{1 + \mu\frac{\beta}{\gamma}(\frac{\alpha\beta}{\gamma\zeta} - 1)N} \right] MN \\
I_1 &= \left[ \eta_I \frac{\kappa_1}{\epsilon_I} \frac{\frac{\beta}{\gamma}}{1 + \mu\frac{\beta}{\gamma}(\frac{\alpha\beta}{\gamma\zeta} - 1)N} - \frac{\lambda_1}{\epsilon_I} \frac{1}{1 + \nu M} \right] \left( \frac{\alpha\beta}{\gamma\zeta} - 1 \right) MN.
\end{aligned}$$

Unlike the system without carrying capacities, this system has stable fixed points without predation, so we may compare populations with and without predation. There are parameter regimes in which only amphibians, or only insects, benefit from the predation. There is also a regime in which predation hurts both species, for instance when both species are bad at metabolizing each other. This situation is essentially a prisoner's dilemma; both species would benefit from a truce, but once a system of reciprocal predation has evolved, it is hard to see how it could stop. Finally, there is a parameter regime where the predation benefits both species by improving the efficiency with which the entire tadpole-frog-insect system uses environmental resources. We will call this a regime of population increase by mutual predation, or PIMP, and we now look at this regime in further detail.

#### 4.1.2 Population increase by mutual predation

Suppose the two types of predation occur with relative strengths given by  $K = \frac{\lambda}{\kappa}$ . We consider turning on predation with fixed  $K$ , so the signs of the total derivatives of  $T$ ,  $F$ , and  $I$  with respect to  $\kappa$  (or  $\lambda$ ) dictate whether predation increases or decreases the population biomasses at equilibrium. When  $\epsilon$  is small,

$$\frac{dT}{d\kappa} = \frac{\partial T_1}{\partial \kappa_1} + K \frac{\partial T_1}{\partial \lambda_1} + O(\epsilon^2),$$

and likewise for the other populations. Evaluated at  $\kappa = 0$ , just as predation is turned on,

$$\begin{aligned}
\left. \frac{dT}{d\kappa} \right|_0 &\sim \frac{1}{\gamma} \left[ K \eta_F \frac{\beta}{\zeta} \frac{1}{1 + \nu M} - \frac{2\frac{\alpha\beta}{\gamma\zeta} - 1}{\frac{\gamma}{\beta} + \mu(\frac{\alpha\beta}{\gamma\zeta} - 1)N} \right] MN \\
\left. \frac{dF}{d\kappa} \right|_0 &\sim \frac{1}{\gamma} \left[ K \eta_F \frac{\gamma}{\zeta} \frac{1}{1 + \nu M} - \frac{\frac{\alpha}{\zeta}}{\frac{\gamma}{\beta} + \mu(\frac{\alpha\beta}{\gamma\zeta} - 1)N} \right] MN \\
\left. \frac{dI}{d\kappa} \right|_0 &\sim \frac{1}{\epsilon_I} \left( \frac{\alpha\beta}{\gamma\zeta} - 1 \right) \left[ \frac{\eta_I}{\frac{\gamma}{\beta} + \mu(\frac{\alpha\beta}{\gamma\zeta} - 1)N} - K \frac{1}{1 + \nu M} \right] MN.
\end{aligned}$$

The signs of the above derivatives determine whether predation hurts or helps a species, insofar as its equilibrium biomass decreases or increases. The regime of PIMP could be defined by the condition that both species' biomasses increase with predation, or by the stronger condition that all three populations' biomasses increase, and it is not obvious which definition is more useful. Biologically, the advantage of a larger population is that it is more fit because it is more genetically diverse and robust to catastrophe. In that sense, it does not matter what life stage the amphibians are in because one life

stage begets another, and our two-stage model is a simplification anyway. On the other hand, it could still be catastrophic for an entire generation of tadpoles to be wiped out. We will thus derive the conditions for PIMP using both the strong and weak definitions.

#### 4.1.3 Conditions for strong population increase by mutual predation

All three derivatives with respect to  $\kappa$  are positive, meaning the equilibrium biomasses of insects and both amphibian life stages increase, if and only if

$$\frac{\zeta}{\beta} \left( 2 \frac{\alpha\beta}{\gamma\zeta} - 1 \right) \text{ and } \frac{\alpha}{\gamma} < K\eta_F \left[ \frac{\frac{\gamma}{\beta} + \mu \left( \frac{\alpha\beta}{\gamma\zeta} - 1 \right) N}{1 + \nu M} \right] < \eta_I \eta_F.$$

By the assumption that  $\frac{\alpha\beta}{\gamma\zeta} > 1$ ,  $\frac{\alpha}{\gamma} < \frac{\zeta}{\beta} \left( 2 \frac{\alpha\beta}{\gamma\zeta} - 1 \right)$ , so strong PIMP occurs if and only if

$$\frac{\zeta}{\beta} \left( 2 \frac{\alpha\beta}{\gamma\zeta} - 1 \right) < K\eta_F \left[ \frac{\frac{\gamma}{\beta} + \mu \left( \frac{\alpha\beta}{\gamma\zeta} - 1 \right) N}{1 + \nu M} \right] < \eta_I \eta_F. \quad (16)$$

The ratio of predation rates,  $K$ , and the rate of reproduction,  $\beta$ , can be changed by behavior, so they can vary on much shorter time scales than the other parameters, which are controlled by physiology. Thus, we may regard  $K$  and  $\beta$  as control parameters. Recalling that  $\zeta = \beta - \epsilon_T$ , it is clear from Equations (13) and (14) that without predation, changing the birth rate cannot increase frog and tadpole populations simultaneously; only predation can do that. There exists an interval of  $K$  in which strong PIMP occurs precisely when

$$\frac{\zeta}{\beta} \left( 2 \frac{\alpha\beta}{\gamma\zeta} - 1 \right) < \eta_I \eta_F. \quad (17)$$

For this inequality to hold, it is necessary that metabolic losses not be too large, and also that  $\alpha < \gamma$  and  $\beta > \zeta$ . That is, predation can only increase all three equilibrium biomasses when frogs gain biomass through their interaction with the external environment, while tadpoles lose it. The biological interpretation of this parameter regime is that frogs are more fit for their environment than tadpoles. Indeed, one could expect this to be true; there are morphogenetic tradeoffs between juvenile and adult fitness, and since frogs spend the majority of their lives in the adult stage, it is likely that they would evolve to be maximally fit as adults. It is less clear that tadpoles would be so unfit as to lose biomass without a constant input from reproduction, but this is certainly feasible in harsh environments that create high juvenile mortality. So, in such a regime, predation can increase all three biomasses by increasing the ratio of frog biomass to tadpole biomass, with insects profiting as middlemen.

#### 4.1.4 Conditions for weak population increase by mutual predation

Let  $A \equiv T + F$ , the total amphibian biomass. Without predation, the equilibrium amphibian biomass is

$$A_0 = \left( \frac{\beta + \gamma}{\gamma} \right) \left( \frac{\alpha\beta}{\gamma(\beta - \epsilon_F)} - 1 \right) N.$$

There is an optimal birth rate,  $\beta$ , that maximizes  $A_0$ . In the strong definition of PIMP there is no such way to define an optimal  $\beta$  since there is always a tradeoff between  $T$  and  $F$ . When  $\beta$  is above its optimal value, too much of the frogs' biomass is going into tadpoles, who are less fit than the frogs. When  $\beta$  is below its optimal value, the frog

population becomes so large than environmental pressures make frogs less successful than tadpoles.

The dependence of equilibrium amphibian biomass on weak predation is

$$\left. \frac{dA}{d\kappa} \right|_0 \sim \frac{1}{\gamma} \left[ K\eta_F \frac{\beta + \gamma}{\zeta} \frac{1}{1 + \nu M} - \frac{2\frac{\alpha\beta}{\gamma\zeta} - 1 + \frac{\alpha}{\zeta}}{\frac{\gamma}{\beta} + \mu\left(\frac{\alpha\beta}{\gamma\zeta} - 1\right)N} \right] MN.$$

Weak predation increases the equilibrium values of both  $A$  and  $I$ , thus satisfying the definition of weak PIMP, if and only if

$$2\frac{\alpha\beta}{\gamma\zeta} - 1 + \frac{\alpha}{\zeta} < K\eta_F \left( \frac{\beta + \gamma}{\zeta} \right) \left[ \frac{\frac{\gamma}{\beta} + \mu\left(\frac{\alpha\beta}{\gamma\zeta} - 1\right)N}{1 + \nu M} \right] < \eta_I \eta_F \left( \frac{\beta + \gamma}{\zeta} \right),$$

and clearly such a  $K$  exists if and only if

$$2\frac{\alpha\beta}{\gamma\zeta} - 1 + \frac{\alpha}{\zeta} < \eta_I \eta_F \left( \frac{\beta + \gamma}{\zeta} \right). \quad (18)$$

This condition is harder to interpret biologically than the stronger condition of Equation (eq: strong PIMP necessary), but it has roughly the same necessary conditions; in the parameter regime for which predation improves efficiency, the metabolisms cannot be too inefficient, frogs cannot be too unfit, and tadpoles cannot be too fit.

Adding predation is like decreasing the rate of reproduction in that it transfers biomass from tadpoles to frogs, though it is certainly not identical. We have not fully explored the relationship between optimal  $\beta$  and optimal  $K$ , but this would be a good topic for future work. For instance, we would like to know whether Equation (18) can hold when the reproduction rate is at its no-predation optimal value, and how the optimal reproduction rate changes in the presence of predation.

#### 4.1.5 Beyond weak predation

We have seen analytically that there is a parameter regime in which PIMP occurs when predation is weak, but we would like to know whether increasing the strength of the predation will increase the equilibrium populations indefinitely. We have not tackled this question analytically, but in all numerical experiments the populations reach a maximum value before decreasing as predation is strengthened further. To use MATCONT, we prefer to work with dimensionless parameters, so we apply the nondimensionalization of Equation (4), the same one used for the system without carrying capacities.

$$\dot{T} = -T + F - d \frac{IT}{1 + T} \quad (19)$$

$$\dot{F} = aT - bF \left( 1 + \frac{1}{N} F \right) + g \frac{FI}{1 + I} \quad (20)$$

$$\dot{I} = cI \left( 1 - \frac{1}{M} I \right) + e \frac{IT}{1 + T} - f \frac{FI}{1 + I}, \quad (21)$$

where  $M$  and  $N$  have been nondimensionalized in the same way as  $I$  and  $F$ , respectively.

In terms of dimensionless quantities, the regime of strong PIMP given by Equation (16) becomes

$$(2a - b) \frac{d}{g} < \frac{1 + \left(\frac{a}{b} - 1\right)N}{1 + M} < \frac{e}{f}.$$

An example case that falls in this regime has  $(a, b, c) = (2, 1, 1)$ ,  $(M, N) = (1, 1)$ , and the predation parameters in fixed proportion such that  $e = 2d$ ,  $f = d$ , and  $g = 4d$ . Figure 6



displays the variation of equilibrium populations with predation strength. Starting with no predation and increasing the predation parameters in fixed proportion, we initially see increases in all three equilibrium populations, as predicted by the asymptotic analysis, followed by decreases in all three populations. Insect population appears to go to zero as predation goes to infinity, while frog and tadpole populations appear to decrease asymptotically to the same finite value. Although it might be possible for the amphibians to predate the insects to extinction, it is not in their interest to do so; this strategy does not maximize their equilibrium population.

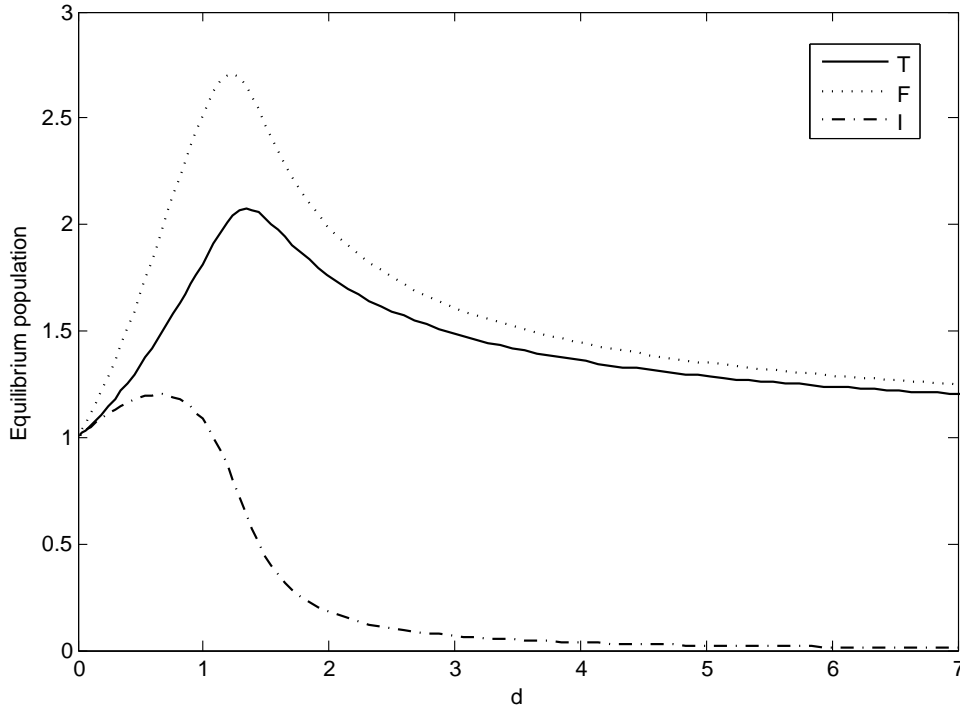


Figure 6: Equilibrium populations as predation strength is varied in the strong PIMP regime. Fixed parameters parameters are  $(a, b, c) = (2, 1, 1)$  and  $(M, N) = (1, 1)$ . Predation parameters are varied in constant proportion with  $e = 2d$ ,  $f = d$ , and  $g = 4d$ .

## 4.2 Numerical exploration of parameter space

We have searched for bifurcations in parameter space using MATCONT, but we have not found any in regimes where PIMP occurs; we simply observe the equilibrium changing its coordinates while remaining stable. In other parameter regimes we find supercritical Hopf bifurcations but no saddle-node bifurcations. The Hopf bifurcations observed in this system were of a different character than those in the system without carrying capacities. In that system, continuing in parameter space past a Hopf bifurcation typically led to growing oscillations and, ultimately, extinction. In the system with carrying capacities, a limit cycle may appear and grow as we move through a Hopf bifurcation, but as we continue through parameter space, it ultimately shrinks and disappears back into a stable equilibrium. So, it seems limit cycles occur only in isolated regions of parameter space where certain resonances are strong. This significant qualitative dif-

ference from the system without carrying capacities is due to the damping effect of the carrying capacities.

## 5 Conclusions

In the model without carrying capacities, we examined the regime in which the insect and frog-tadpole systems decay without predation. Predation can create stable fixed points and limit cycles, though the limit cycles are not robust and rather unrealistic biologically, so in this model the two species are completely codependent. For this stabilization to occur, predation must be above a certain minimum strength, and the relative strengths of insect-tadpole and frog-insect predation must be within a certain interval. There are biological parameters for which a fixed point and a limit cycle are simultaneously stable, but we have not found parameters for which nontrivial stable fixed points coexist.

In the model with carrying capacities, both species exist stably without predation. Depending on the biological parameters, predation may increase or decrease the equilibrium populations in any combination. Fixing all biological parameters other than predation rates, we have seen that mutual predation can increase all of the equilibrium populations simultaneously. However, there always exists an optimal rate of reproduction that maximizes the equilibrium biomass of amphibians, and we have not determined whether predation can only increase all populations simultaneously by effectively decreasing the rate of reproduction toward its optimal value. If this is the case, we must ask whether it is biologically realistic for the amphibians to habitually reproduce at a non-optimal rate, and if not, we would conclude that population increase by mutual predation is not biologically relevant in the long term. This is both a mathematical and biological question for future study.

## 6 Acknowledgments

I would like to thank all the staff members of the 2010 GFD program who had helpful discussions with me over the summer, particularly Charles Doering, Antonello Provenzale, and Glenn Flierl, who between them gave me constant guidance on this project.

## 7 Appendix: The Holling type II functional form

The simplest system in which the Holling type II functional form could appear is a 2D predator-prey model. However, the justification for using this specific form in such a model is not clear *a priori*. A quadratic predation term that is proportional to both predator and prey populations would not require much justification since it represents leading order behavior at the very least, but such a term produces unrealistic exponential growth in the system. However, building on the work of Whitehead and Doering [4], we can create a dichotomy between hungry predators sated predators and use only linear and quadratic terms in the resulting 3D system, and then find that in the appropriate limit it reduces to a 2D predator-prey system with Holling type II predation laws. The functional forms of the 3D model do not require justification since they are the simplest laws that could capture the necessary behavior. To evaluate the accuracy of the reduced system with Holling type II laws, we shall compare its features to those of the full 3D system.

## 7.1 The 3D system

The 3D system consists of hungry predator ( $H$ ), sated predators ( $S$ ), and prey ( $P$ ):

$$\begin{aligned}\dot{H} &= -\phi PH + \mu S - \delta H + \beta S \\ \dot{S} &= \phi PH - \mu S - \delta S \\ \dot{P} &= -\phi PH + \gamma P \left(1 - \frac{P}{n}\right).\end{aligned}$$

Hungry predators eat prey at rate  $\phi$  and become sated predators, while sated predators metabolize and become hungry at rate  $\mu$ . Both hungry and sated predators die at rate  $\delta$ , and sated predators give birth to hungry ones at rate  $\beta > \delta$ . The prey is being born according to a logistic law. In a more accurate model, the  $\phi$  and  $\delta$  constants in the different equations could take different values, but this would only add parameters without changing any qualitative results.

To reduce the order of the system, we will consider the limit of large metabolism rate, i.e.  $\mu \gg \beta, \delta, \gamma$ . To see how each variable should scale with  $\mu$ , we consider the three-species equilibrium,

$$(H_0, S_0, P_0) = \left(\frac{\gamma}{\phi}, \frac{\gamma}{\phi} \frac{\delta}{\beta - \delta}, \frac{\mu + \delta}{\phi} \frac{\delta}{\beta - \delta}\right).$$

At equilibrium, there is  $O(\mu)$  more prey than predators. This motivates us to scale the prey variable in  $\mu$ , so we nondimensionalize the system by

$$H \mapsto \frac{\delta}{\phi} h \quad S \mapsto \frac{\delta}{\phi} s \quad P \mapsto \frac{\delta}{\phi} X \quad t \mapsto \frac{1}{\delta} \tau.$$

The nondimensional 3D system is

$$\begin{aligned}\dot{h} &= -\frac{1}{\epsilon} X h + \frac{1}{\epsilon} s - h + b s \\ \dot{s} &= \frac{1}{\epsilon} X h - \frac{1}{\epsilon} s - s \\ \dot{X} &= -X h + g X \left(1 - \frac{X}{N}\right),\end{aligned}$$

where

$$\begin{aligned}b &\equiv \frac{\beta}{\delta} > 1 \\ g &\equiv \frac{\gamma}{\delta} \\ \epsilon &\equiv \frac{\delta}{\mu}.\end{aligned}$$

We shall consider the singular limit where a predator eats many times in its life, i.e.  $\epsilon \ll 1$ . The parameter  $b$  is the ratio of predator birthrate to death rate,  $g$  is the ratio of prey birthrate to predator death rate, and  $N$  is the dimensionless carrying capacity of the environment for prey. Note that predator and prey populations are in different units, so their numerical values can not be meaningfully compared.

## 7.2 Reduced systems

The 3D system's behavior can only be well approximated by a two dimensional system if its behavior is roughly two dimensional, for instance this implies that it must not be chaotic. There must be a two-dimensional slow manifold in phase space on which all solutions approximately lie, possibly after some transient behavior as the component of the solution on the fast manifold rapidly decays. Reduction of order is achieved by

projecting the full system onto the slow manifold. To find the slow manifold, we observe that the system is linear in  $h$  and  $s$  if  $X$  is regarded as a known function of time:

$$\begin{pmatrix} \dot{h} \\ \dot{s} \end{pmatrix} = \begin{pmatrix} -(\frac{1}{\epsilon}X + 1) & \frac{1}{\epsilon} + b \\ \frac{1}{\epsilon}X & -(\frac{1}{\epsilon} + 1) \end{pmatrix} \begin{pmatrix} h \\ s \end{pmatrix}.$$

The eigenvalues of this system are

$$\lambda_{\pm} = -\frac{1}{\epsilon} \frac{X+1}{2} - 1 \pm \frac{1}{\epsilon} \frac{X+1}{2} \sqrt{1 + \epsilon \frac{4bX}{(X+1)^2}}.$$

To first order in  $\epsilon$ ,

$$\begin{aligned} \lambda_+ &= -1 + \frac{bX}{X+1} + O(\epsilon) \\ \lambda_- &= -\frac{1}{\epsilon}(X+1) - 1 + \frac{bX}{X+1} + O(\epsilon). \end{aligned}$$

The  $\lambda_+$  eigenvalue is  $O(1)$ , while the  $\lambda_-$  eigenvalue is negative and  $O(\frac{1}{\epsilon})$ , so solutions decay quickly along the direction of the  $\lambda_-$  eigenvector and move more slowly in the  $\lambda_+$  direction. Thus at a given  $X$ , the  $\lambda_-$  vector is tangent to the fast manifold, and the  $\lambda_+$  vector is tangent to the slow manifold.

### 7.2.1 Full 2D system

The  $\lambda_+$  eigenvector yields a proportionality between  $s$  and  $h$  on the slow manifold as a function of  $X$ ,

$$s = \frac{1}{2(1+\epsilon b)} \left( X - 1 + \sqrt{(X+1)^2 + 4\epsilon b X} \right) h.$$

This relation may be used to reduce the dynamical system by eliminating either  $h$  or  $s$ , but since we are ultimately concerned with the total number of predators, we define  $Y \equiv h + s$  and work in this variable. Applying the above  $s(h)$  relation to the 3D system, we obtain our 2D reduction,

$$\begin{aligned} \dot{X} &= gX \left( 1 - \frac{X}{N} \right) - \frac{2(1+\epsilon b)XY}{X+1 + \sqrt{(X+1)^2 + 4\epsilon b X} + 2\epsilon b} \\ \dot{Y} &= -Y + \frac{(X-1 + \sqrt{(X+1)^2 + 4\epsilon b X})bY}{X+1 + \sqrt{(X+1)^2 + 4\epsilon b X} + 2\epsilon b}. \end{aligned}$$

### 7.2.2 $O(\epsilon)$ 2D system

If we approximate the  $s(h)$  relation to  $O(\epsilon)$ , we obtain a simpler relation that still captures some affects of finite  $\epsilon$ ,

$$s = \left( X - \epsilon \frac{bX^2}{1+X} \right) h + O(\epsilon^2).$$

The  $O(\epsilon)$  truncated reduced system is

$$\begin{aligned} \dot{X} &= gX \left( 1 - \frac{X}{N} \right) - \frac{XY}{1+X} - \epsilon \frac{bX^3Y}{(X+1)^3} \\ \dot{Y} &= -Y + \frac{bXY}{1+X} - \epsilon \frac{b^2X^2Y}{(X+1)^3}. \end{aligned}$$

### 7.2.3 Holling type II 2D system

If we truncate further and retain only the  $O(1)$  term in  $\epsilon$ ,

$$s = hX + O(\epsilon).$$

Using this simple proportionality we recover the Holling type II functional form.

$$\begin{aligned}\dot{X} &= gX\left(1 - \frac{X}{N}\right) - \frac{XY}{1+X} \\ \dot{Y} &= -Y + \frac{bXY}{1+X}.\end{aligned}$$

The form  $\frac{XY}{1+X}$  goes by various other names in other fields, such as the Jacob-Monod form in microbiology or the Michaelis-Menten form in enzyme kinetics.

## 7.3 Comparison of system behaviors

To understand what has been lost by projecting onto the slow manifold, as well as by truncating in  $\epsilon$ , one must compare the behavior of the full 3D system with the behaviors of the reduced 2D systems. There is no unique measure of the quality of the approximation; different properties are approximated better than others, so the value of the approximation depends ultimately on what properties are of interest.

For the 3D system, we ignore the separate dynamics of the  $h$  and  $s$  variables and consider only their sum,  $Y$ , because this is the quantity of interest and the one that compares directly to the 2D models. As we demonstrate below, all four models have the same qualitative behavior, some representative phase portraits of which are given in Figure 7. There is a trivial equilibrium at the origin representing mass extinction, but it is always unstable. There is a prey-only equilibrium, stable only when  $b$  and  $N$  are small. That is, when predators are not born too fast, and saturation population of prey is not too large, both factors that would inhibit predator success. When  $b$  and  $N$  are a bit larger so conditions are a bit better for predators, the prey-only equilibrium becomes unstable as a stable two-species equilibrium becomes physical and splits off from it in a transcritical bifurcation. The two-species equilibrium is a plain sink initially and becomes a spiral sink at larger  $b$  and  $N$ . When  $b$  and  $N$  are increased further still, the two-species equilibrium undergoes a Hopf bifurcation, losing its stability to a limit cycle. All orbits are bounded for all parameter values. Since all four systems share this qualitative picture, the effects of approximation appear only in the quantitative differences between, say, equilibria and limit cycle locations, or bifurcation values.

### 7.3.1 Equilibria

At all parameter values, all four systems have equilibria at the origin and at  $(X, Y) = (N, 0)$ . Solving for the nontrivial two-species equilibria, we obtain  $Y_0 = \frac{bg}{b-1}\left(1 - \frac{X_0}{N}\right)$  for all four systems, though the  $X_0$  value may vary between systems. Clearly the nontrivial equilibrium is only physical ( $Y_0 > 0$ ) when  $X_0$  is less than  $N$ , the prey-only saturation population. That is, such equilibria never represent mutualistic solutions. The  $X_0$  values for the two-species equilibria in each system are tabulated in Table 2. The  $X_0$  value for the  $O(\epsilon)$  system is more cleanly expressed implicitly by the cubic equation of which it is the only positive real root. The full 2D system has exactly the same equilibrium as the 3D system, while the truncated systems have different two-species equilibria, which converge to the 3D value as  $\epsilon \rightarrow 0$ .

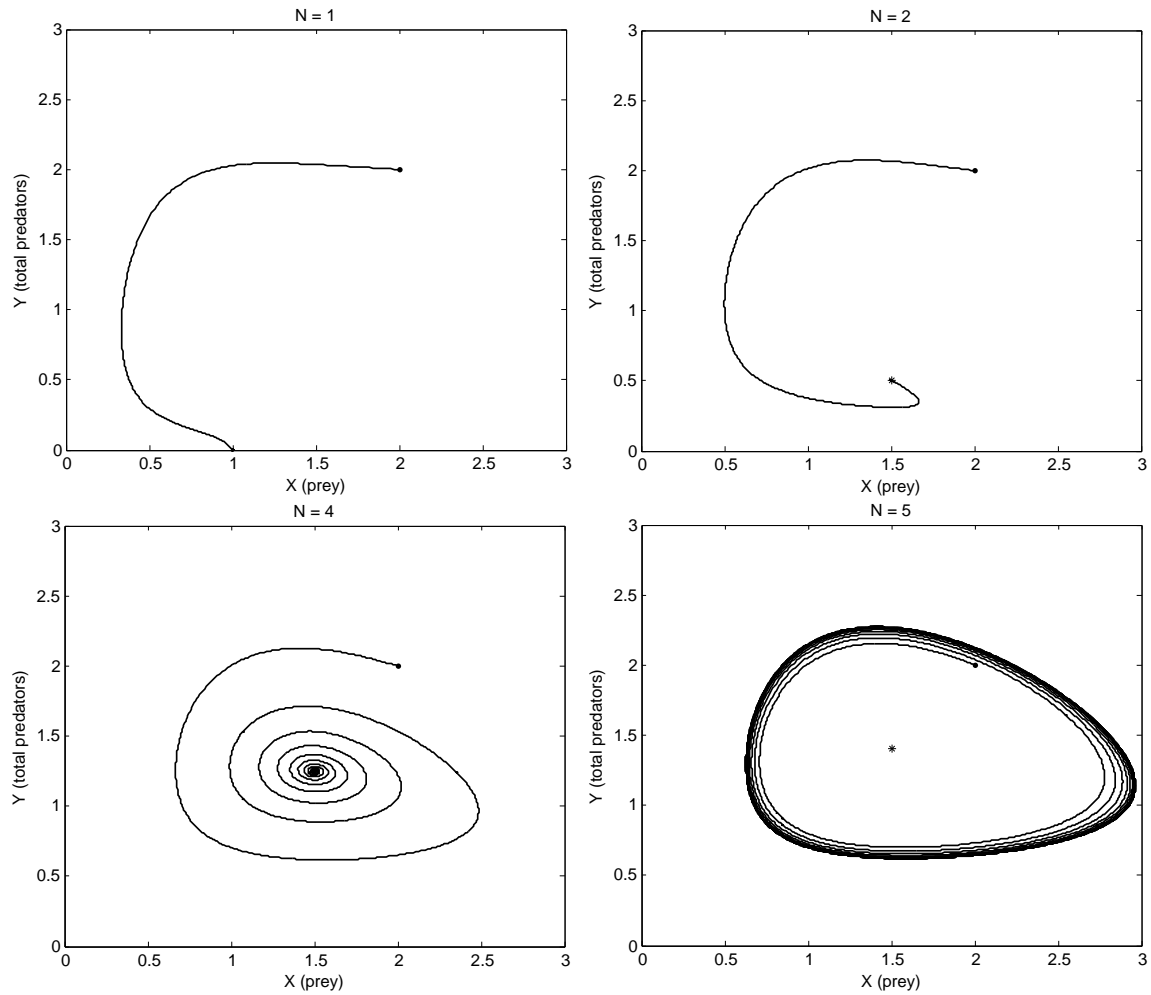


Figure 7: Sample phase portraits representing all four possible qualitative behaviors, considering  $N$  as the control parameter: stable prey-only equilibrium (upper left), stable two-species equilibrium with plain sink (upper right), stable two-species equilibrium with spiral sink (lower left), and a limit cycle around the two-species equilibrium (lower right). These portraits were generated by integrating the 3D system with  $b = 2$ ,  $g = 1$ , and  $\epsilon = 0.5$ .

Table 2: Locations of the two-species equilibria in the four models.

Model	$X_0$	$Y_0$
3D	$\frac{1+\epsilon}{b-1}$	$\frac{bg}{b-1} \left(1 - \frac{1+\epsilon}{N(b-1)}\right)$
Full 2D	$\frac{1+\epsilon}{b-1}$	$\frac{bg}{b-1} \left(1 - \frac{1+\epsilon}{N(b-1)}\right)$
$O(\epsilon)$ 2D	$(b-1)X_0^3 + (2b - \epsilon b^2 - 3)X_0^2 + (b-3)X_0 - 1 = 0$	$\frac{bg}{b-1} \left(1 - \frac{X_0}{N}\right)$
Holling type II 2D	$\frac{1}{b-1}$	$\frac{bg}{b-1} \left(1 - \frac{1}{N(b-1)}\right)$

### 7.3.2 Linear stability

To analyze the linear stability of the three equilibria in all four systems, we linearize each system about an arbitrary point,  $(h_0, s_0, X_0)$ , or  $(X_0, Y_0)$ .

#### 3D system

$$\frac{d}{dt} \begin{pmatrix} \Delta h \\ \Delta s \\ \Delta X \end{pmatrix} = \begin{pmatrix} -(\frac{1}{\epsilon}X_0 + 1) & \frac{1}{\epsilon} + b & -\frac{1}{\epsilon}h_0 \\ \frac{1}{\epsilon}X_0 & -(\frac{1}{\epsilon} + 1) & \frac{1}{\epsilon}h_0 \\ -X_0 & 0 & -h_0 + g(1 - \frac{2X_0}{N}) \end{pmatrix} \begin{pmatrix} \Delta h \\ \Delta s \\ \Delta X \end{pmatrix}$$

#### Full 2D system

$$\frac{d}{dt} \begin{pmatrix} \Delta X \\ \Delta Y \end{pmatrix} = \begin{pmatrix} m_{XX} & m_{XY} \\ m_{YX} & m_{YY} \end{pmatrix} \begin{pmatrix} \Delta X \\ \Delta Y \end{pmatrix}, \text{ where}$$

$$m_{XX} = g\left(1 - \frac{2X_0}{N}\right) - \left(1 - \frac{X_0}{\sqrt{(X_0+1)^2 + 4\epsilon b X_0}}\right) \frac{2(1+\epsilon b)Y_0}{1+X_0 + \sqrt{(X_0+1)^2 + 4\epsilon b X_0} + 2\epsilon b}$$

$$m_{XY} = \frac{2(1+\epsilon b)X_0}{1+X_0 + \sqrt{(X_0+1)^2 + 4\epsilon b X_0} + 2\epsilon b}$$

$$m_{YX} = \left(\frac{b}{\sqrt{(X_0+1)^2 + 4\epsilon b X_0}}\right) \frac{2(1+\epsilon b)Y_0}{1+X_0 + \sqrt{(X_0+1)^2 + 4\epsilon b X_0} + 2\epsilon b}$$

$$m_{YY} = -1 - \frac{1}{2\epsilon}(X_0 + 1 + \sqrt{(X_0+1)^2 + 4\epsilon b X_0})$$

#### $O(\epsilon)$ 2D system

$$\frac{d}{dt} \begin{pmatrix} \Delta X \\ \Delta Y \end{pmatrix} = \begin{pmatrix} g\left(1 - \frac{2X_0}{N}\right) - \frac{Y_0}{(1+X_0)^2} - \epsilon \frac{3bX_0^2 Y_0}{(1+X_0)^4} & -\frac{X_0}{1+X_0} - \epsilon \frac{bX_0^3}{(1+X_0)^3} \\ \frac{bY_0}{(1+X_0)^2} + \epsilon \frac{b^2(X_0^2 - 2X_0)Y_0}{(1+X_0)^4} & \frac{bX_0}{1+X_0} - 1 - \epsilon \frac{b^2 X_0^2}{(1+X_0)^3} \end{pmatrix} \begin{pmatrix} \Delta X \\ \Delta Y \end{pmatrix}$$

#### Holling type II 2D system

$$\frac{d}{dt} \begin{pmatrix} \Delta X \\ \Delta Y \end{pmatrix} = \begin{pmatrix} g\left(1 - \frac{2X_0}{N}\right) - \frac{Y_0}{(1+X_0)^2} & -\frac{X_0}{1+X_0} \\ \frac{bY_0}{(1+X_0)^2} & \frac{bX_0}{1+X_0} - 1 \end{pmatrix} \begin{pmatrix} \Delta X \\ \Delta Y \end{pmatrix}$$

About the origin, every linearized system has an eigenvalue of  $g$ , which is positive, so the extinction equilibrium is always unstable. Linearizing about the prey-only equilibrium, one finds that each system goes unstable according to the same parameter

inequalities that determine when the two-species equilibrium exists. This is as expected from a transcritical bifurcation; the stability of the prey-only equilibrium changes precisely when it collides with the two-species equilibrium, which is also the moment when that equilibrium becomes physical. As for the two-species equilibrium, we can study its stability analytically in the Holling type II system, but the other linearized systems are messy, so we solve their stability eigenproblems numerically.

### 7.3.3 Stability of the two-species equilibrium in the Holling type II 2D system

The Holling type II system linearized about its two-species equilibrium is

$$\frac{d}{dt} \begin{pmatrix} \Delta X \\ \Delta Y \end{pmatrix} = \begin{pmatrix} \frac{g}{b} \left(1 - \frac{b+1}{N(b-1)}\right) & -\frac{1}{b} \\ g(b-1 - \frac{1}{N}) & 0 \end{pmatrix} \begin{pmatrix} \Delta X \\ \Delta Y \end{pmatrix}.$$

The stability of the two-species equilibria is not hard to compute analytically for the Holling type II system. The characteristic equation of the linearized system is

$$\lambda^2 - \frac{g}{b} \left(1 - \frac{b+1}{N(b-1)}\right) \lambda + \frac{g}{b} \left(b-1 - \frac{1}{N}\right) = 0.$$

For the two-species equilibrium to exist, the  $O(1)$  coefficient of the characteristic equation must be positive. Thus, solving the quadratic equation for  $\lambda$ , the discriminant will either be imaginary or of smaller magnitude than the  $O(\lambda)$  coefficient. Either way, both eigenvalues will be negative (the equilibrium will be stable) if and only if the  $O(\lambda)$  coefficient is positive, i.e. when  $N < \frac{b+1}{b-1}$ . When  $N$  exceeds this value, all three equilibria are unstable. We later prove that all orbits are bounded, so the Poincaré-Bendixon theorem will guarantee that the system converges to a limit cycle.

### 7.3.4 Bifurcations

The transcritical bifurcation occurs when  $Y_0$  exceeds zero, which occurs when the  $X_0$  expressions reported in Table 2 are less than  $N$ . For each system, this is possible only when  $b > 1$ . The exact relation between  $b$  and  $N$  at the bifurcations are given in Table 3. Note that from a point in parameter space where the prey-only equilibrium is stable, the bifurcation may be produced by increasing either  $b$  or  $N$ . The point in parameter space where the Hopf bifurcation occurs has a simple analytic expression for the Holling type II model, so this is also given in Table 3. For the other models, the  $N$  at which the Hopf bifurcation occurs was computed numerically for given values of  $b$ ,  $g$  and  $\epsilon$ , and some representative results are plotted in Figure 8. The 3D transcritical bifurcation depends only on  $b$ ,  $N$  and  $\epsilon$ , while the Hopf bifurcation depends also on  $g$ , but quite weakly so. It is clear from Figure 8 that the full 2D model captures the transcritical bifurcation perfectly, while the truncated models are inaccurate when  $\epsilon$  becomes large. At the Hopf bifurcation, the full 2D model captures the 3D behavior imperfectly, but again much better than the truncated models.

### 7.3.5 Lyapunov stability

Each system undergoes only the two bifurcations we have studied and has no other fixed points. All that remains is to verify that in each system the orbits are bounded for all parameter values. We shall do this by the Lyapunov method for the 3D system and the Holling type II 2D system. We shall not prove boundedness for the other two systems, whose algebraic nonlinearities would make it a cumbersome task, but we can feel confident in its veracity.



Table 3: Bifurcation points of the four models. For the  $O(\epsilon)$  model,  $X_0$  is defined implicitly by the formula given in Table 2.

Model	Transcritical bifurcation	Hopf bifurcation
3D	$0 < \frac{1+\epsilon}{b-1} \leq N$	Found numerically
Full 2D	$0 < \frac{1+\epsilon}{b-1} \leq N$	
$O(\epsilon)$ 2D	$0 < X_0 \leq N$	
Holling type II 2D	$0 < \frac{1}{b-1} \leq N$	$\frac{b+1}{b-1} \leq N$

**Holling type II 2D system** Examining the  $\dot{X}$  equation, we see that  $\dot{X} < 0$  whenever  $X > N$ . Thus, if  $X < N$  at the initial condition, it remains true for all time. To put an upper bound on  $Y$  that is valid for all parameters, we must consider  $X$  and  $Y$  together in a Lyapunov functional.

Let  $L \equiv X + \frac{1}{b}Y$ . The proportionality between  $X$  and  $Y$  is chosen such that the nonlinear Holling type II terms in  $\dot{L}$  cancel:

$$\dot{L} = gX\left(1 - \frac{X}{N}\right) - \frac{1}{b}Y.$$

Our goal is to bound  $\dot{L}$  by an affine function of  $L$ , i.e.  $\dot{L} \leq \alpha - \beta L$ , where  $\beta > 0$ . This will imply that  $L < \frac{\alpha}{\beta}$  for all time if it is true initially. To bound  $\dot{L}$  by such a term we must bound the quadratic  $X$  term by an affine function of  $X$  with a negative coefficient on  $X$ . Any line tangent to the parabola at  $X_* > \frac{N}{2}$  will suffice, but we seek the line that minimizes  $\frac{\alpha}{\beta}$ , thereby providing the optimal bound on  $L$ . An arbitrary tangent line gives the bound

$$X\left(1 - \frac{X}{N}\right) \leq \frac{X_*^2}{N} - \left(\frac{2X_*}{N} - 1\right)X,$$

which induces a bound on  $\dot{L}$ ,

$$\dot{L} \leq \frac{X_*^2}{N} - \min\left\{\frac{2X_*}{N} - 1, \frac{1}{b}\right\}L.$$

Thus,

$$L < \inf_{X_* > N/2} \frac{X_*^2}{N \min\left\{\frac{2X_*}{N} - 1, \frac{1}{b}\right\}}.$$

Assuming the above infimum occurs at an  $X_*$  such that  $\frac{2X_*}{N} - 1 < \frac{1}{b}$ , the optimal choice of  $X_*$  in fact contradicts the assumption when  $b > 1$ . So, the minimum must be  $\frac{1}{b}$ , meaning that  $X_* \geq \frac{N}{2}\left(1 + \frac{1}{b}\right) \geq N$ . The bound on  $L$  then becomes

$$L < \inf_{X_* \geq \frac{N}{2}\left(1 + \frac{1}{b}\right)} \frac{bX_*^2}{N} = \frac{N}{4b}(b+1)^2.$$

Putting this in terms of  $X$  and  $Y$ , and adding the known bound on  $X$  alone,

$$X < \min\left\{\frac{N}{4b^2}(1+b)^2 - \frac{1}{b}Y, N\right\}.$$

**3D system** Let  $L \equiv h + \alpha s + \beta X$ . To make the  $hX$  terms to vanish from  $\dot{L}$ , we let  $\beta = \frac{\alpha-1}{\epsilon}$ , which clearly requires  $\alpha > 1$  for  $\beta$  to be positive. Thus,

$$\begin{aligned} \dot{L} &= -\left[\frac{1}{\epsilon} + 1 - \left(\frac{1}{\epsilon} + b\right)/\alpha\right]\alpha s - h + \frac{1}{\epsilon}(\alpha-1)gX\left(1 - \frac{X}{N}\right) \\ &\leq -m(\alpha)L + \frac{1}{\epsilon}(\alpha-1)X\left[\left(g + m(\alpha)\right) - \frac{gX}{N}\right], \end{aligned}$$

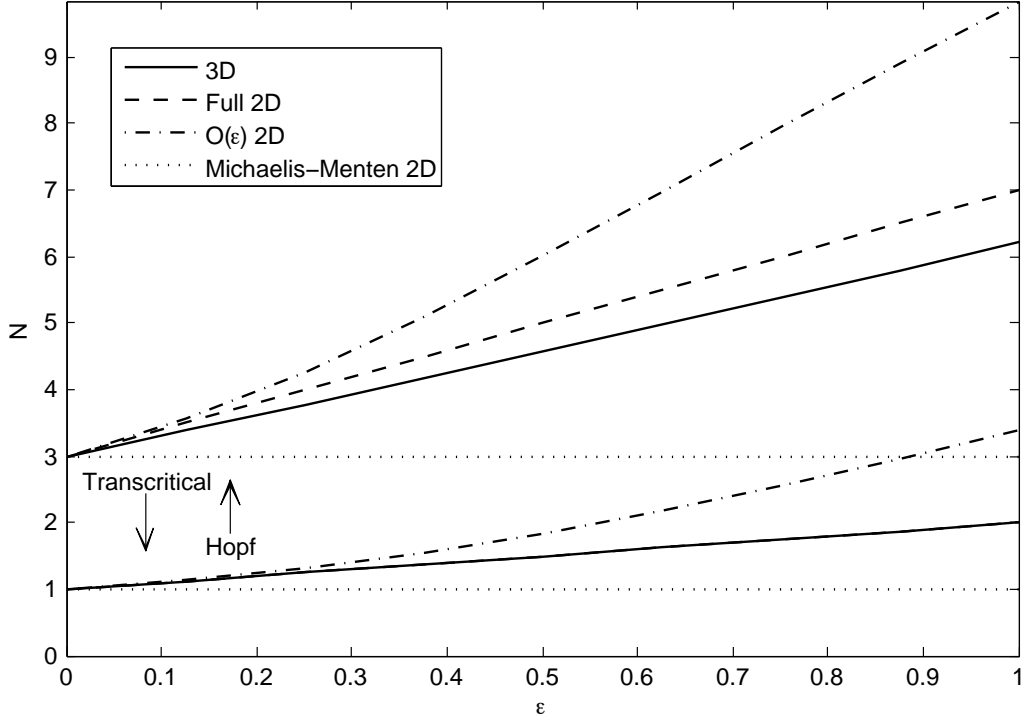


Figure 8: Values of  $N$  as a function of  $\epsilon$  at the transcritical and Hopf bifurcations for all four systems with  $b = 2$  and  $g = 1$ . For the transcritical bifurcation, the full 2D systems coincides with the 3D system.

where  $m(\alpha) \equiv \min \left\{ 1, \frac{1}{\epsilon} + 1 - \left( \frac{1}{\epsilon} + b \right) / \alpha \right\}$ . We now bound the quadratic  $X$  term by its maximum value without bothering to find the optimal bound linear in  $X$ .

$$\dot{L} \leq -m(\alpha)L + \frac{N}{4\epsilon g}(\alpha - 1)(g + m(\alpha))^2.$$

This yields a bound on  $L$  that can be optimized over all allowable  $\alpha$ :

$$L < \inf_{\alpha > 1} \frac{N}{4\epsilon g} \frac{\alpha - 1}{m(\alpha)} (g + m(\alpha))^2.$$

Assuming the infimum occurs when  $m(\alpha) = 1$  implies that the optimal bound is obtained by choosing  $\alpha = 1^+$ , which contradicts  $m(\alpha) = 1$ . Let  $\alpha \geq \frac{1+\epsilon b}{1+\epsilon}$ , giving our best result for a bound on the Lyapunov functional:

$$L < \inf_{\alpha \geq \frac{1+\epsilon b}{1+\epsilon}} \frac{N}{4\epsilon^2 g} \frac{\alpha - 1}{1 + \epsilon - \frac{1+\epsilon b}{\alpha}} \left( g + 1 + \epsilon - \frac{1+\epsilon b}{\alpha} \right)^2.$$

The optimal bound can be calculated given the other parameters, but the more important conclusion is that some such finite bound always exists for  $L$ .

### 7.3.6 Summary of results

Our analysis strongly suggests that  $X$  and  $Y$  have the same qualitative behavior in all four systems, though to make this result rigorous, one needs Lyapunov bounds on the

full 2D and  $O(\epsilon)$  2D systems, and one needs to show analytically that a Hopf bifurcation occurs in all systems as it does in the Holling type II system. Trusting that the systems indeed all have the same behavior, they differ only quantitatively. We have seen that the full 2D system has the same two-species equilibrium as the 3D system, while the truncated systems do not, and quantitative differences in bifurcation values were shown already in Figure 8.

Phase portraits produced by the different models appear in Figure 9. Although the 2D systems began with the same initial conditions, we must compare them each to their own corresponding 3D solution because they each correspond to slightly different decompositions of  $Y_0$  into  $h_0$  and  $s_0$ . However, the three 3D solutions tend to be quite similar. The top row of Figure 9 shows solutions at small  $N$ , when the prey-only equilibrium is stable. The prey-only equilibrium is identical in all four systems, so the phase portraits agree well even for  $\epsilon = 0.5$ . The middle row of Figure 9 shows solutions for larger  $N$ , when the two-species equilibrium is stable. The different systems agree well when  $\epsilon$  is 0.05, but at 0.5 the locations of the equilibria differ significantly, so the respective phase trajectories spiraling towards them are quantitatively quite different. The bottom row of Figure 9 shows long-time solutions at still larger  $N$ . When  $\epsilon$  is 0.05, the limit cycles of the full 2D and  $O(\epsilon)$  2D systems approximate the 3D limit cycle quite well, while the Holling type II system does a bit worse. When  $\epsilon$  is 0.5, the Holling type II system's limit cycle is much too large, the full 2D system's is too small but a bit better, and the  $O(\epsilon)$  2D system has not yet gone through the Hopf bifurcation.

The full 2D system approximates the 3D system well for  $\epsilon \lesssim 0.5$ , while the Holling type II 2D system is quantitatively accurate only when  $\epsilon$  is an order of magnitude smaller. We wish to extrapolate these truths to other models where the Holling type II or full-order-in- $\epsilon$  functional forms might be used as predation laws without repeating their rigorous derivation from a higher-order dynamical system. If  $\epsilon$  is very small, or if one is only concerned with qualitative features, as is often the case in biological modeling, the Holling type II functional form is certainly satisfactory. If  $\epsilon$  is closer to unity, and the quantitative properties of the system matter, as is often the case in enzyme kinetics, the full-order-in- $\epsilon$  functional form would be a better choice. The  $O(\epsilon)$  functional form probably offers neither enough simplicity nor accuracy to be chosen over the other two.

## References

- [1] C. S. HOLLING, *Some characteristics of simple types of predation and parasitism*, Canadian Entomologist, (1959).
- [2] E. E. WERNER AND J. F. GILLIAM, *The ontogenetic niche and species interactions in size-structured populations*, Ann. Rev. Ecol. Syst., (1984).
- [3] J. P. WHITEHEAD AND C. R. DOERING, *Notes on some age structure trophic dynamics*, (2007, unpublished).
- [4] ———, *Simple hungry and satiated predator*, (2007, unpublished).

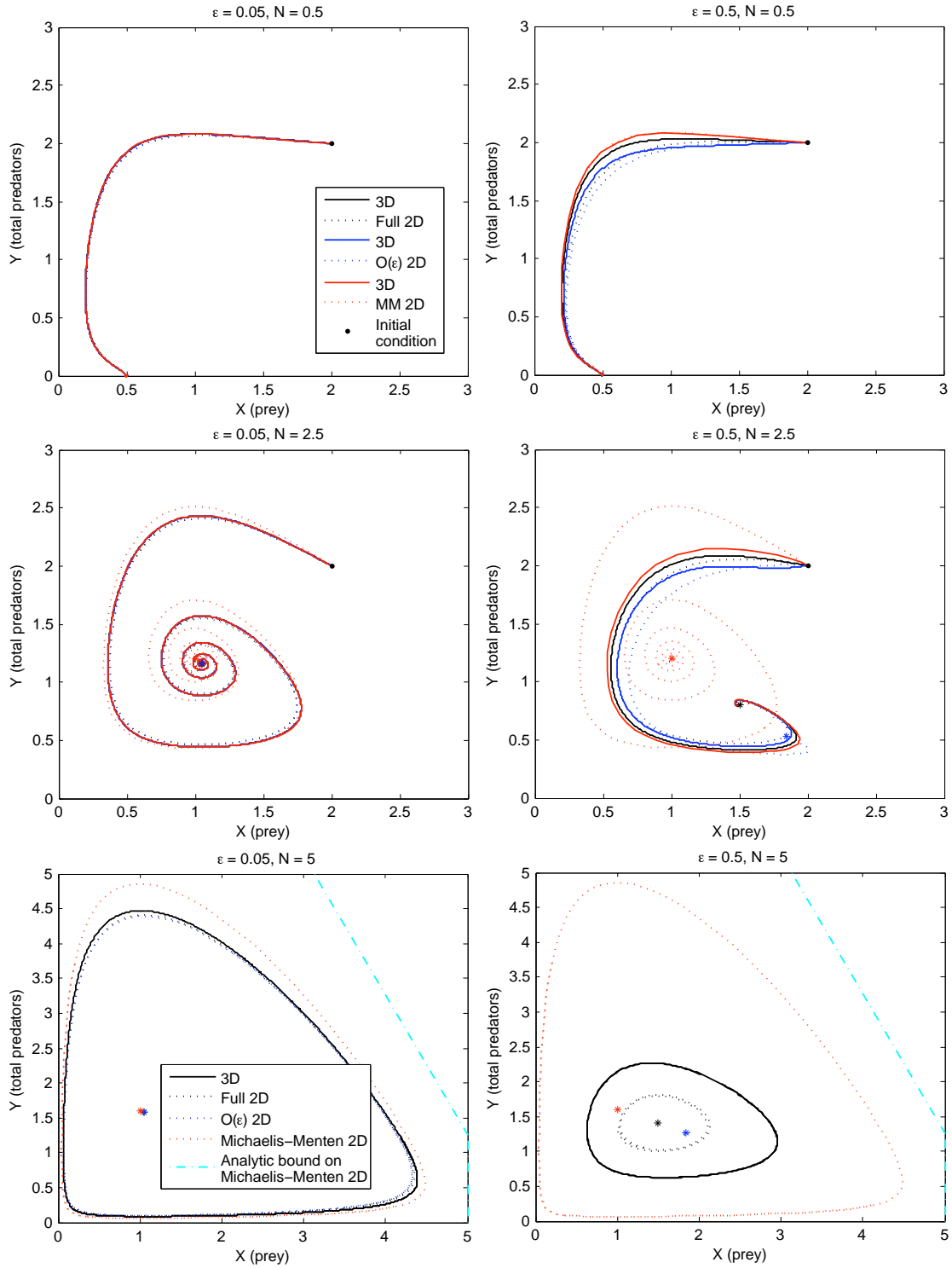


Figure 9: Phase portraits of all four systems for values of  $N$  with  $\epsilon = 0.05$  (left) and  $\epsilon = 0.5$  (right), and  $b = 2$ ,  $g = 1$ . All solutions began at  $(2,2)$ , but only the late-time behavior is shown in the bottom two plots to make the limit cycles clear. The asterisks are the equilibria of the different systems, which always coincide for the 3D system and the full 2D system.